METHODS

A New Method to Localize Acid Phosphatase Using the Confocal Laser-Scanning Microscope

Zsolt SZEGEDI,[1] Farhana AMIN,[2] Béla SZENDE,[1] Ivor Delme BOWEN[2]

[1]1st Institute of Pathology and Experimental Cancer Research, Department of Molecular Pathology, Joint Research Organization of the Hungarian Academy of Sciences and Semmelweis University of Medicine, Budapest, Hungary, [2]Department of Pure and Applied Biology, University of Cardiff, Cardiff, Wales, UK

The aim of the study was to develop a technique for the detection of acid phosphatase enzyme activity by confocal laser-scanning microscope using the histochemical acid phosphatase detection method (after Barka and Anderson 1962, modified by Bowen and Lewis 1985) routinely used for light microscopy. The density and the distribution of enzyme reaction product is dependent on the incubation time, as shown by different confocal images or ELISA reader. The inhibition of the enzyme activity with metal ions shows the same profile known from the literature. This staining method seems to be useful to demonstrate subcellular distribution of the enzyme in the lysosomes and in the Golgi apparatus. (Pathology Oncology Research Vol 4, No 3, 217–223, 1998)

Key words: acid phosphatase activity; cytometry; cell image analysis; confocal laser-scanning microscope

Introduction

Acid phosphatase (AcPhase) is normally transported from the site of synthesis to the ER, Golgi and lysosomes as a membrane-bound enzyme. The transport to the lysosomes is independent of mannose-6-phosphate receptor, usually a key element for the transport of lysosomal enzymes. The cytoplasmic domain of AcPhase contains a GY-motif (glycine-tyrosine), which is essential for lysosomal transport (a so-called lysosomal targeting signal). During the transport the enzyme is modified by different proteases and loses 30% of its molecular weight.[1] Based on ultrastructural studies the enzymatic activity is localized in distal Golgi cisternae, condensed vacuoles, primary and secondary lysosomes.[2]

Modulation of AcPhase levels and formation occurs in various pathological conditions. Moderate elevations in total enzyme level were observed in cases of thromboembolic phenomena, thrombocytopenia, multiple myeloma, liver disease and Paget's disease. Increased AcPhase activity was reported in feeding yeast[3] during programmed cell death in metamorphosing insects and other organisms[4,5,6,7] and in human prostate cancer during progression and in colon cancer cells after tyrphostin treatment.[8,9,10] The importance of the localization of AcPhase justifies those efforts establishing novel, simpler but comparatively accurate methodologies. Therefore, the aim of our study was to apply laser-scanning microscopy for the cytochemical analysis of AcPhase at cellular levels using the modified Barka and Anderson method.[11,12,13]

Methods

Cell cultures

The UA hybridoma cell line (murine L929 fibrosarcoma (ATCC number: CRL-2148), human U939 myelomonocytic leukemia (ATCC number: CRL-9591) from Dr. N. Matthews) and the HT-29 human colon adenocarcinoma cell line (ATCC number: CCL-218) were cultured in 24-well Greiner (Kremsmünster, Austria) plates using RPMI medium (Sigma) containing 10% fetal calf serum (Sigma). The cell number/ml was 2×10^5 and 10^5, respectively. Enzyme incubation started 36 hours after plating. After removal of medium and washing with PBS the glass coverslip-adherent cells were dried at room temperature or at
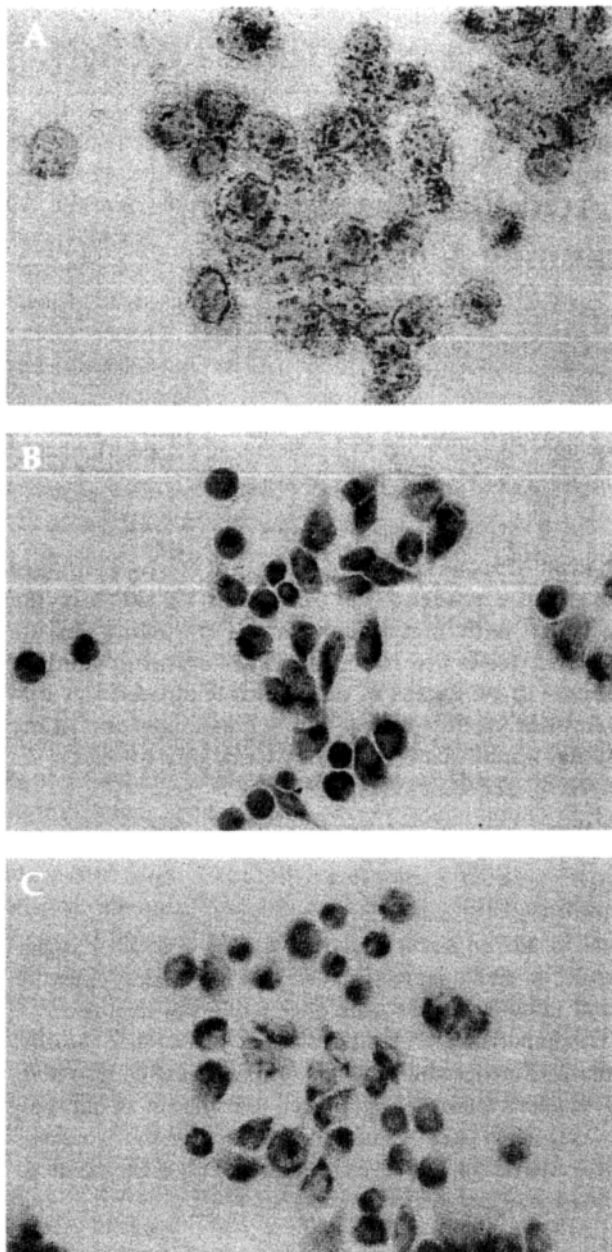
Figure 1. Light microscopic picture of acid phosphatase distribution. A: Native cells, only the reaction product can be seen. B: Hematoxilin nuclear staining. C: Methyl-green counterstain.

56°C, 37°C and 4°C, respectively. One coverslip of each sample was fixed with absolute methanol and another one with 2.5% glutaraldehyde.

Histochemical detection of AcPhase[9,10]

Chemicals: Naphthol AS-BI Phosphate (Sigma), Fast Red Violet (Sigma), Manganese chloride (Sigma). The following basic solutions were prepared for 30 ml reaction mixture: 500 mM $MnCl_2$ (10 ml), 0.7 mM Naphthol AS-BI phosphate (20 ml, dissolved in pH 4.7 acetate buffer), 32 mM Fast Red Violet (1 ml). The detection method was based on the following chemical reaction:[14]

Naphthol AS-BI Phosphate + H_2O → α -Naphthol + P_I
α-Naphthol + Diazonium salt → Azo dye
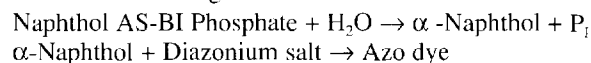
The naphthol derivative couples with the unstable diazonium salt, to produce a red azo dye at the site of enzyme activity, which is detectable with light microscope as small, red azo dye particles in the cytoplasm.

Incubation, counterstain

The three solutions were mixed just before reaction. ptt was checked and adjusted to 4.7 by HCl. One of the samples was treated with the reaction mixture at pH 9.5. Another sample contained $ZnSO_4$ (5 mM) to inhibit the enzymatic activity. The slides were covered with the reaction mixture, stored in humidified box at 37°C and incubated for different periods (15, 30, 60, 90, 120 and 180 min, respectively). The mixture was removed and the slides were washed with distilled water. After washing the samples were put into PBS for 15 min. Hematoxylin or methyl-green nuclear staining was used for light microscopy.

For confocal microscopy, propidium iodine and acridine orange (concentration for each was 7.5 µM) was used as DNA markers on two samples (the others contained the product of enzyme reaction only) and wet mounted by Cityfluor (Montreal).

Confocal microscopy

To visualize the cells and AcPhase reaction products, a Bio-Rad confocal laser-scanning microscope (MRC-1024, Bio-Rad, London, UK) was used. The following parameters were applied to obtain images:

For azo dye fluorescence (AcPhase reaction), the argon laser was used at 647 nm and the emission filter was 585
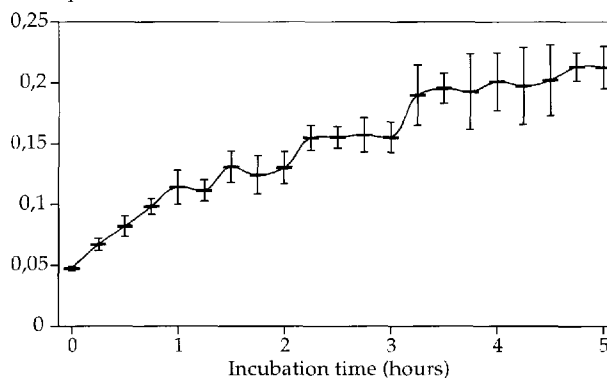

Figure 2. Analysis of different incubation times with ELISA reader.
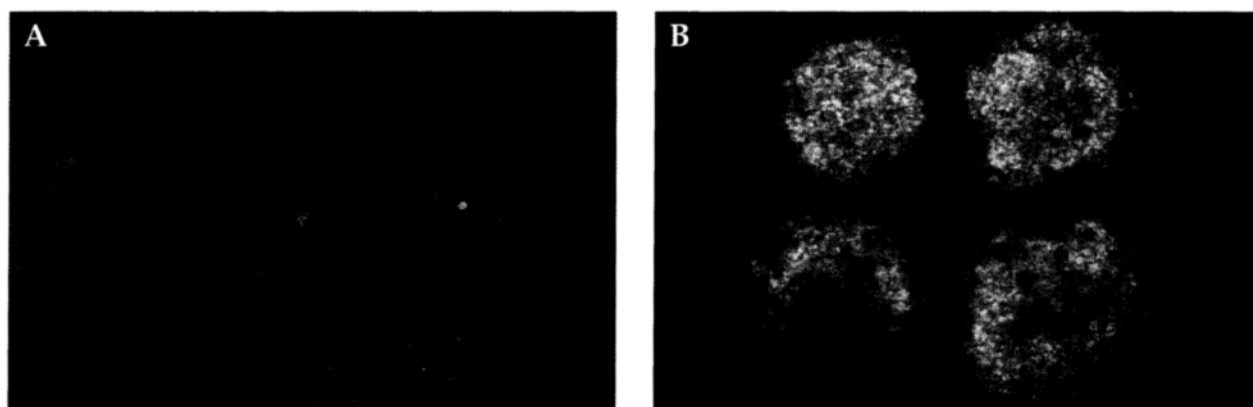
Figure 3. The acid phosphatase reaction and propidium iodide nuclear stain. Two different coloring methods. A: The nuclei are red and the reaction product is green. B: The propidium iodide signal is green and the reaction product is red.

EFLP. For the propidium iodine signal (DNA) the laser was set for all lanes and the emission filter was left open. Occasionally the cell's green autofluorescence was also detected separately (laser filter).

Inhibition of AcPhase with metal ions

Each salt concentration was 0.2 mM. Each compound was applied simultaneously in the reaction mixture. Incubation time was 3 hours followed by 30 min incubation in 1% sodium dodecyl sulfate (SDS, Sigma). The inhibitory effect was measured by ELISA reader (LabTech Multiskan-M) at 405 nm. The inhibitory effect of the following compounds on AcPhase was studied: manganese (II) chloride ($MnCl_2$), zinc sulfate ($ZnSO_4$), lead acetate ($Pb(CH_3COO)_2$), calcium chloride ($CaCl_2$), cupric sulfate ($CuSO_4$), ferric chloride ($FeCl_3$), magnesium chloride ($MgCl_2$), cobalt chloride ($CoCl_2$), sodium molybdate (Na_2MoO_4) and sodium fluoride (NaF).

Time dependency of enzyme reaction

Different incubation times were employed in order to assess the dynamics of the enzyme reaction. A 96-well Greiner plate (Kremsmünster, Austria) was used. In each well 100 µl medium contained 2×10^5 cells. The reactions in four samples were stopped every 15 minute by washing in PBS up to 5 hours. Air dried cells were incubated in 1% sodium dodecyl sulfate (SDS, Sigma L5901). The reaction product was measured by ELISA as above.

Results

The cells studied by light microscopy, which were incubated for 3 hours with the substrate, showed a diffuse strong red reaction product in the cytoplasm *(Figure 1A)*. Using methyl-green counterstain, both cytoplasm and the nuclei

could be identified *(Figure 1C)*, but the hematoxylin nuclear stain seems also to be adequate because the high density of enzyme reaction marks the cytoplasm *(Figure 1B)*.

The production of azo dye in the fixed cells is time-dependent according to the ELISA measurement, where the maximum is reached at 3.5 hours *(Figure 2)*. For confocal imaging 15 min incubation seems to be enough to mark the lysosomal enzymes but the sites of low enzyme activity remain hidden at this point. Propidium iodine staining resulted in a clear nuclear staining without disturbing the enzyme reaction *(Figure 3A, B)*.

Zn^{2+}, Cu^{2+}, Fe^{3+}, Mo^{6+} and F ions inhibited AcPhase activity significantly (p<0.005) compared to control cells *(Figure 4)*. Other ions like Pb^{2+}, Mg^{2+}, Co^{2+}, Ca^{2+} and Mn^{2+} did not inhibit the enzyme activity in accordance with the literature.[15]

Acridine orange produced high background and its fluorescence competed with the azo dye. *(Figure 5A)*. Acetone fixation preserved both structure and enzyme
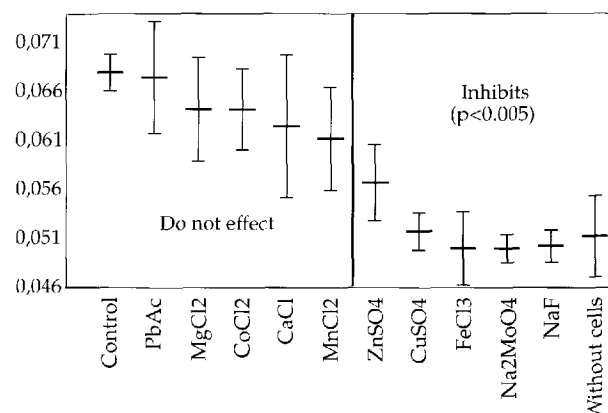
Absorption at 405 nm

Figure 4. Inhibition of acid phosphatase activity with different ions. Measured by an ELISA-reader at 405 nm.
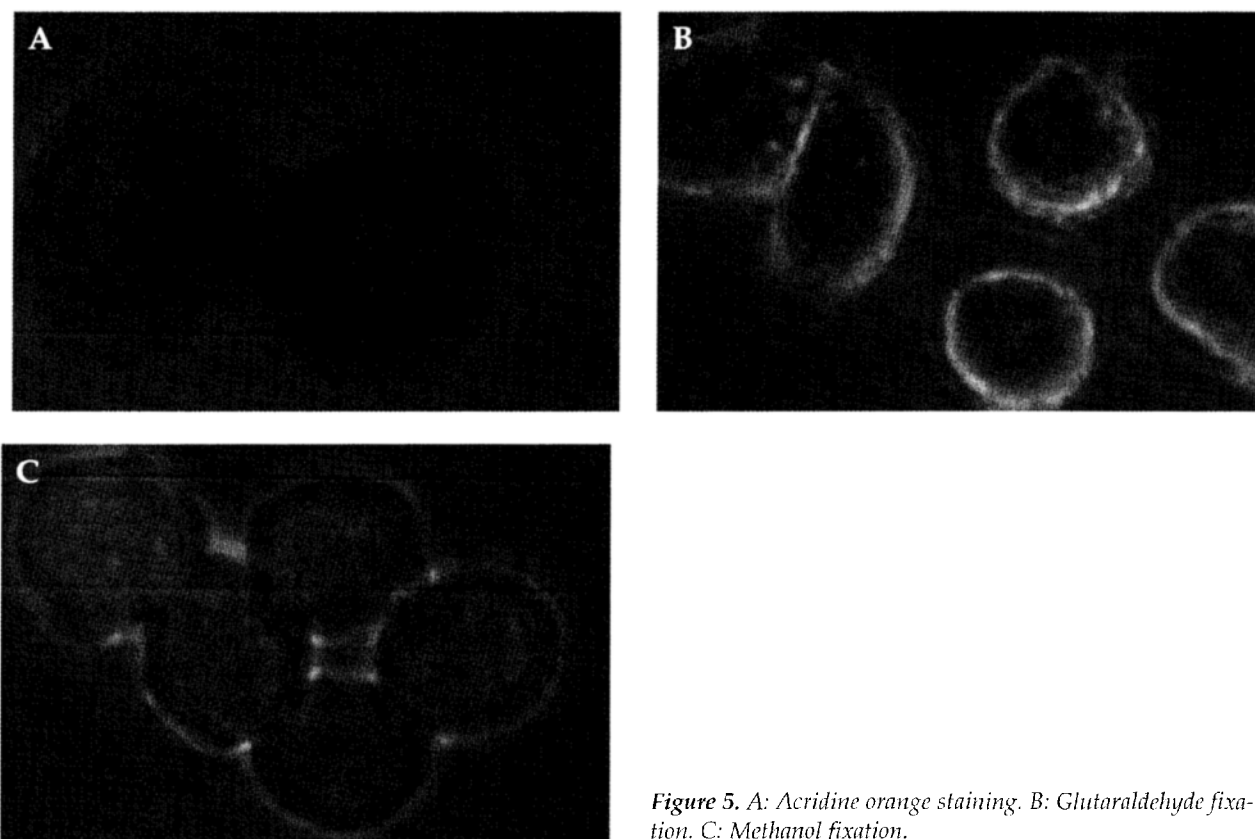
Figure 5. A: Acridine orange staining. B: Glutaraldehyde fixation. C: Methanol fixation.

activity, while glutaraldehyde fixation produced strong background fluorescence and methanol seems to denature AcPhase activity (Figure 5B, 5C). The quality of images does not depend on the duration of air-drying. Incubation at 56°C for 30 minutes does not inhibit the enzyme activity.

Various visualization methods were tried for confocal microscopy. When the AcPhase reaction product was colored red, surrounded by green autofluorescence, the additive signal appeared to be yellow. In some image layers (including 0.1 μm thin section) homogenous distribution of the reaction product could be seen (Figure 6A). Depending on the position of the sectioning, in the presence of positively stained Golgi structure polarity of the cell could be determined. In the case of post-mitotic cells this polarity was always observed in the neighboring side of the daughter cells (Figure 6B). Using phase-contrast imaging (gray) as complementary information,
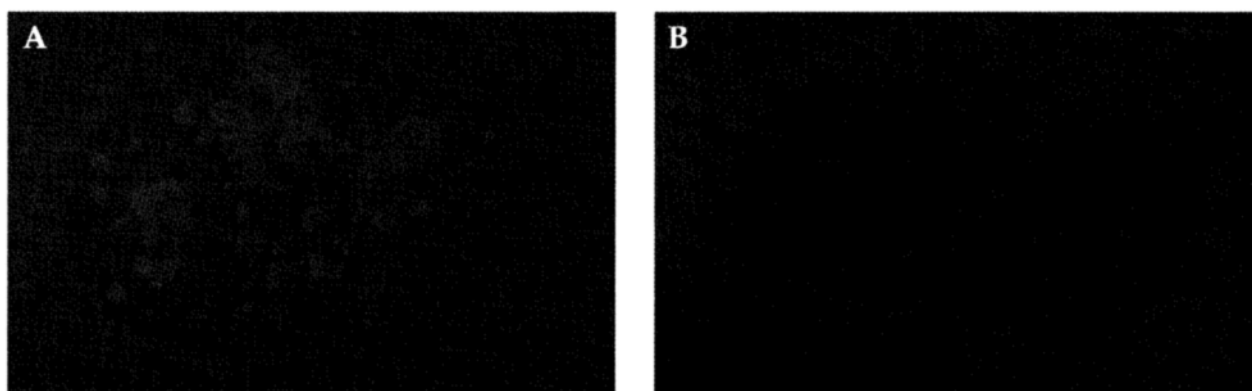

Figure 6. Confocal laser-scanning image of HT-29 human colon carcinoma cell, 15 min incubation. The gray background derives from phase-contrast view. A: Lower section (close to the plate surface). B: Higher section with lot of surrounding intra cytoplasmic signs.
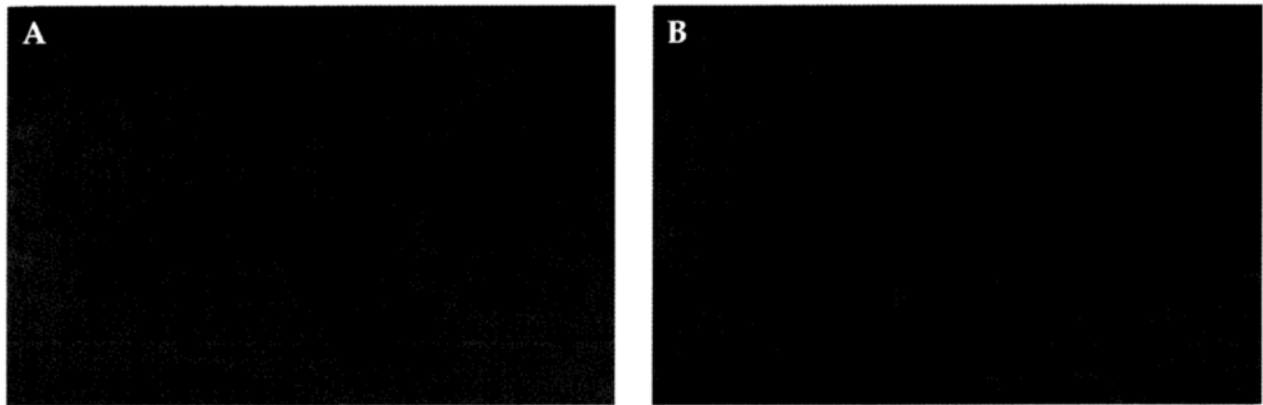
Figure 7. *Single layer sections from HT-29 cells. The side-preference of acid phosphatase activity is shown.*

the heterogeneous distribution of enzyme reaction represented by variable density of acphase positive grains could be seen depending on the height of investigated layer. The red reaction product was condensed at the opposite side to the plate surface *(Figure 7A, B)*. After 15 min incubation time the enzyme product showed a more homogenous distribution around the nucleus. This incubation time seems to be enough to "stain" the lysosomes but insufficient to visualize the Golgi cisternae. After 1–3 hours of incubation the balance between the lysosomal and Golgi localization of AcPhase changes in favour of Golgi and reveals a polarized localization *(Figure 8A, B)*.

Sometimes, the reaction appears as groups of grains *(Figure 9A)*. At higher magnification, these grains form rosettes and the intracellular localization is usually close to the nucleus *(Figure 9B)*.

The best images were achieved when propidium iodine was used as gray nuclear background and the reaction product was presented as red. At a lower magnification the cells show polarity based on the density of the reaction

product *(Figure 10A, B)*. When the optical sections were superimposed and presented as single image this cytoplasmic polarity appeared around the AcPhase-negative nucleus *(Figure 10C)*.

Discussion

Detection of AcPhase at cellular level is an important cell biological and histopathological problem. At light microscopy level it is well established, but the simplicity of the reaction is associated with poor subcellular resolution. However, high resolution is associated with complex and complicated electron microscopic methodology. Obviously, it would be an advantage to combine the simplicity with higher subcellular resolution. We found, that the conventional AcPhase reaction using azo dye as endproduct can be applied to confocal microscopy since the end-product has fluorescency at 405 nm. Because the optical sectioning significantly improves the resolution, the localization of the enzymatic activity is almost as accurate as in the electron microscopic method.
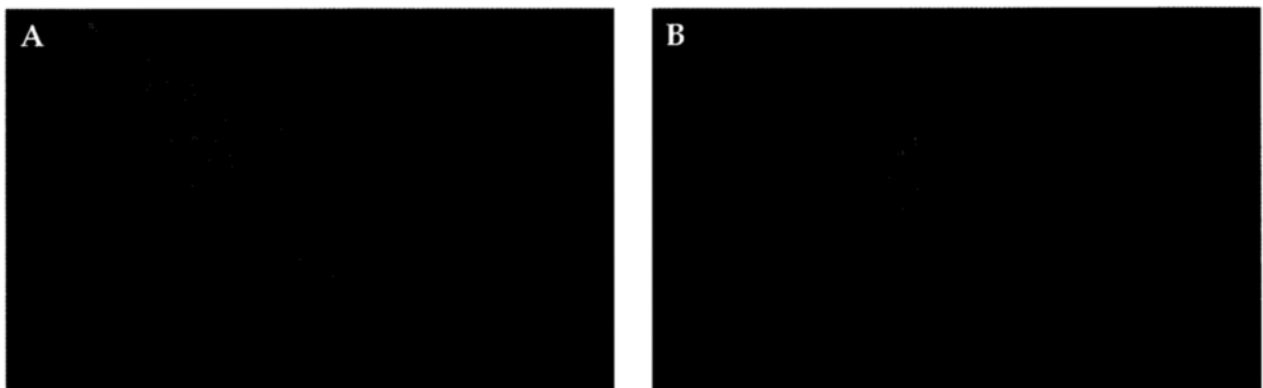

Figure 8. *Confocal laser-scanning image of human-mouse hybridoma cells. A: Red azo dye in the cytoplasm shows the localization of acid phosphatase activity. The green color derives from autofluorescence. B: Newly divided cells. Most of the reaction products appear on the neighbouring side of the daughter cells.*
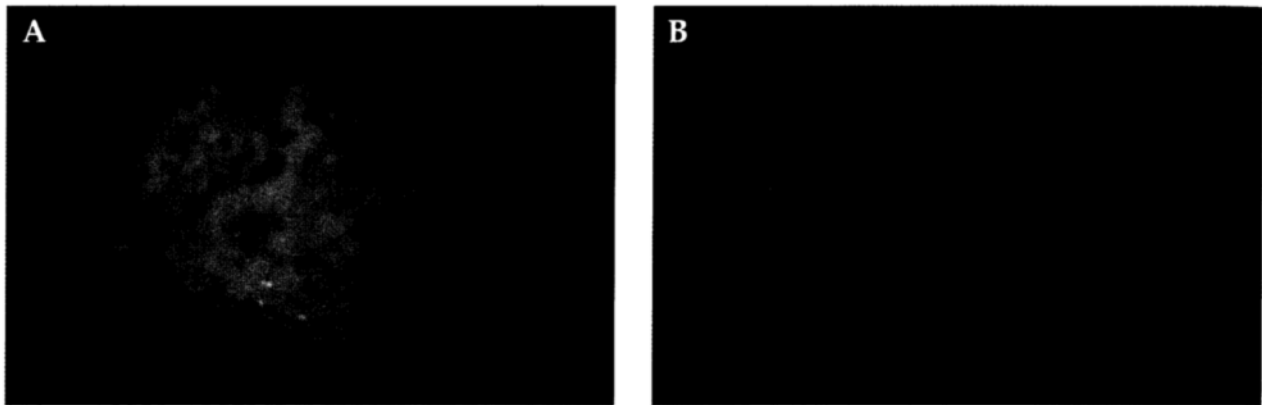
Figure 9. Acid phosphatase reaction product and propidium iodide nuclear stain. The nucleus is green and the reaction product is purple. A: Single cell with intensive enzyme activity. B: The same cell at higher magnification. The reaction product in some places grouping like a rosette.

The level of the reaction product of modified Barka and Anderson method showed good correlation with incubation time. This reaction could be inhibited by ions which are usually inhibitors of acid phosphatase enzyme *in vitro*. The confocal localization of acid phosphatase achieved in tumor cells agrees well with the data presented by Sarraf and Bowen[16] on S180 murine sarcoma using the Barka and Anderson method with Naphthol AS TR phosphate as substrate and hexazonium pararosani-

line as coupler. They also observed transient increases in acid phosphatase activity in dying cells. We are planning to compare the AcPhase enzyme reaction product with immunohistochemical detection of AcPhase using specific antibodies or EM using various substrates.[17] This may provide information on the localization of active and inactive forms of the enzyme, including the hypothetical free cytoplasmic subtype.[18]
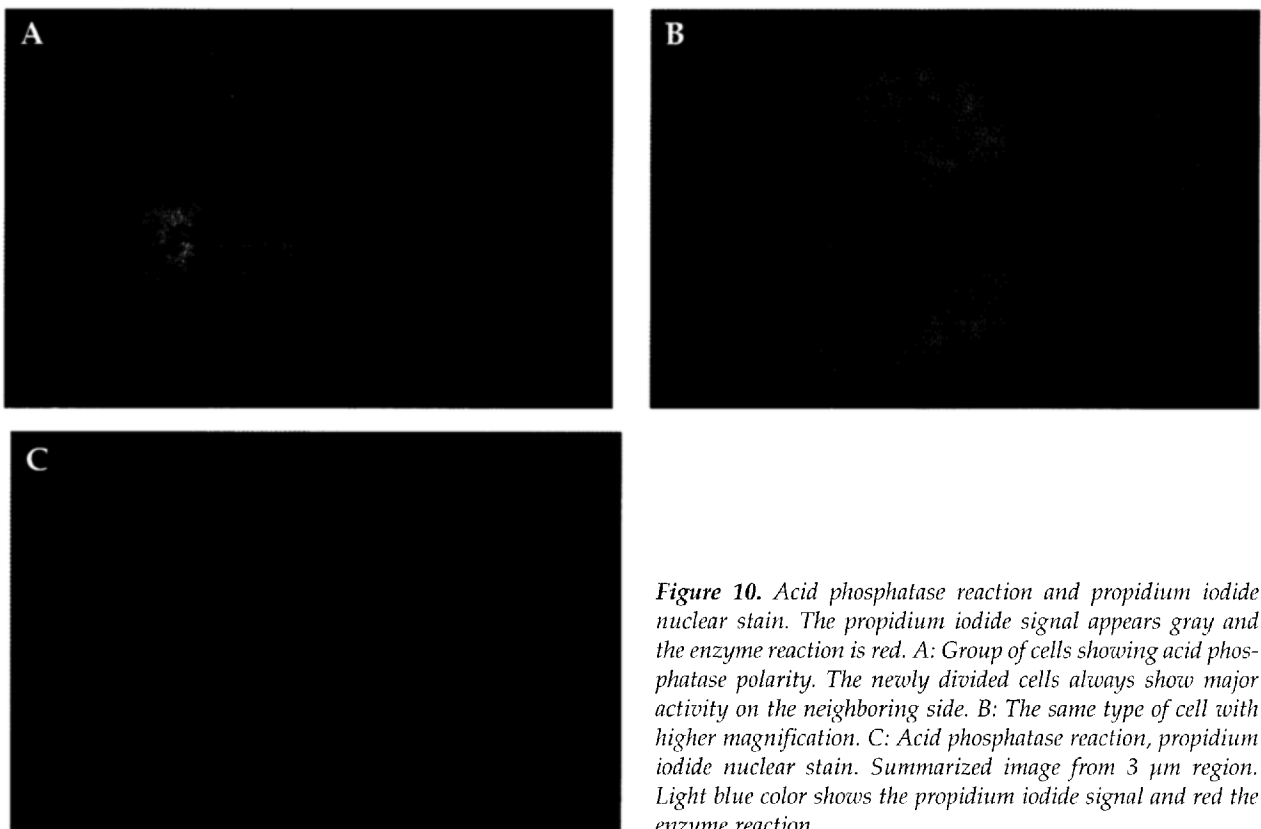

Figure 10. Acid phosphatase reaction and propidium iodide nuclear stain. The propidium iodide signal appears gray and the enzyme reaction is red. A: Group of cells showing acid phosphatase polarity. The newly divided cells always show major activity on the neighboring side. B: The same type of cell with higher magnification. C: Acid phosphatase reaction, propidium iodide nuclear stain. Summarized image from 3 µm region. Light blue color shows the propidium iodide signal and red the enzyme reaction.

References

1. *Himeno M, Tanaka Y:* Biosynthesis, processing, and lysosome targeting of acid phosphatase. Nippon-Rinsho 53:2898-2903, 1995.
2. *Fujita H, Okamoto H:* Fine structural localization of thiamine pyrophosphatase and acid phosphatase activities in the mouse pancreatic acinar cell. Histochemistry 64:287-295, 1979.
3. *Ramoino P, Beltrame F, Fato M:* Image analysis of lysosomal activity during the early clonal life of Paramecium primaurelia. FEMS Microbiol Letters 125:57-62, 1995.
4. *Bowen ID, Mullarkey K, Morgan SM:* Programmed cell death during metamorphosis in the blow-fly Calliphora vomitoria. Microscopy Research and Technique 34:202-217, 1996.
5. *Bowen ID, den Hollander JH, Lewis GHJ:* Cell death and acid phosphatase activity in the regenerating planarian Polycelis tenuis. Differentiation 21:160-167, 1982.
6. *Bowen ID, Lewis GHJ:* Histochemical applications of X-ray microanalysis: the simultaneous assessment of mitosis and cell death using an X-ray microanalytical method in the scanning electron microscope SEM. IV SEM Inc. AMF O'Hare, Illinois, pp. 179-187, 1980.
7. *Bowen ID, Ryder TA:* Use of the p-nitrophenyl phosphate method for the demonstration of acid phosphatase during star-

vation and cell autolysis in the planarian Polycelis tenuis Iijima. Histochem J 8:319-329, 1976.
8. *Szende B, Kéri Gy, Szegedi Zs, et al:* Clarke type III programmed cell death of tumour cells induced by a tyrosine kinase inhibitor. Cell Proliferation 28:188, 1995.
9. *Szegedi Zs, Kéri Gy, Benedeczky I, et al:* Inducibility and possible mechanism of Clarke III type programmed cell death in human carcinoma cell lines. Cell Biology International 20:233, 1996.
10. *Szegedi Zs, Sleták A, Nagy J, et al:* Characterisation of cell death caused by the tyrphostin AG-213 on human cell lines. Cell Proliferation 29:283, 1996.
11. *Barka T, Anderson PJ:* Histochemical methods for acid phosphatase using hexazonium pararosanilin as coupler. J Histochem Cytochem 10:741, 1962.
12. *Lewis GHJ, Bowen ID:* A methacrylate embedding technique for combined autoradiography and acid phosphatase histochemistry. Histochem J 17:467-475, 1985.
13. *Lojda Z, van der Ploeg M, Duijn P:* Phosphates of the naphthol AS series in the quantitative determination of alkaline and acid phosphatase activities "in situ" studied in polyacrilamide membrane model systems and by cytospectrophotometry. Histochemie 11:13-32, 1967.
14. *Pearse AGE:* Histochemistry, Theoretical and Applied, 2nd ed., Little, Brown & Co., Boston, pp. 882, 1960.
15. *Biswas TK, Promo M, Biswas B:* Purification of acid phosphatase 1 from germinating seeds of Vigna sinensis. Phytochemistry 41:1457-1458, 1996.
16. *Sarraf CE, Bowen ID:* Kinetic studies on murine sarcoma and an analysis of apoptosis. Br J Cancer 54:989-998, 1986.
17. *Ryder TA, Bowen ID:* A method for the fine structural localisation of acid phosphatase activity using p-nitrophenyl phosphate as substrate. J Histochem Cytochem 23:2235-2237, 1975.
18. *Clarke PGH:* Developmental cell death: morphological diversity and multiple mechanisms. Anatomy and Embryology 181:195-213, 1990.